AWARD NUMBER: W81XWH-18-1-0546

TITLE: Developing New Therapeutic Strategies for Malignant Peripheral Nerve Sheath Tumor By Interrupting Immunologic Tolerance

PRINCIPAL INVESTIGATORS: Timothy Cripe, MD, PhD

CONTRACTING ORGANIZATION: The Research Institute at Nationwide Children's Hospital
Columbus, OH

REPORT DATE: December 2021

TYPE OF REPORT: Final

PREPARED FOR: U.S. Army Medical Research and Development Command
Fort Detrick, Maryland 21702-5012

REPORT DOCUMENTATION PAGE

Form Approved
OMB No. 0704-0188

1. REPORT DATE	2. REPORT TYPE	3. DATES COVERED
December 2021	Final	15Aug2018-14Aug2021

4. TITLE AND SUBTITLE

Developing New Therapeutic Strategies for Malignant Peripheral Nerve Sheath Tumor By Interrupting Immunologic Tolerance

5a. CONTRACT NUMBER

5b. GRANT NUMBER
W81XWH-18-1-0546

5c. PROGRAM ELEMENT NUMBER

6. AUTHOR(S)
Timothy Cripe, MD
Kevin Cassady, MD

E-Mail: timothy.cripe@nationwidechildrens.org

5d. PROJECT NUMBER

5e. TASK NUMBER

5f. WORK UNIT NUMBER

7. PERFORMING ORGANIZATION NAME(S) AND ADDRESS(ES)

RESEARCH INSTITUTE AT NATIONWIDE CHILDRENS
700 CHILDRENS DR
COLUMBUS OH 43205-2664

8. PERFORMING ORGANIZATION REPORT NUMBER

9. SPONSORING / MONITORING AGENCY NAME(S) AND ADDRESS(ES)

U.S. Army Medical Research and Development Command
Fort Detrick, Maryland 21702-5012

10. SPONSOR/MONITOR'S ACRONYM(S)

11. SPONSOR/MONITOR'S REPORT NUMBER(S)

12. DISTRIBUTION / AVAILABILITY STATEMENT

Approved for Public Release; Distribution Unlimited

13. SUPPLEMENTARY NOTES

14. ABSTRACT

Based on recent data from us and others using human clinical MPNST specimens, we seek validation in mouse models of a novel treatment paradigm that could lead to new clinical trials. Our approach is based on stimulating antitumor immunity using oncolytic virus infections combined with inhibitors of immunosuppression, including those targeting TGFβ (both directly and indirectly, through the Janus kinase inhibitor Ruxolitinb) and T cell checkpoints.

15. SUBJECT TERMS
None listed.

16. SECURITY CLASSIFICATION OF:			17. LIMITATION OF ABSTRACT	18. NUMBER OF PAGES	19a. NAME OF RESPONSIBLE PERSON
a. REPORT	b. ABSTRACT	c. THIS PAGE			USAMRDC
Unclassified	Unclassified	Unclassified	Unclassified	30	19b. TELEPHONE NUMBER *(include area code)*

TABLE OF CONTENTS

1. INTRODUCTION:

Based on recent data from us and others using human clinical MPNST specimens, we seek validation in mouse models of a novel treatment paradigm that could lead to new clinical trials. Our approach is based on stimulating antitumor immunity using oncolytic virus infections combined with inhibitors of immunosuppression, including those targeting TGFβ (through specific inhibition and indirectly through the Janus kinase inhibitor Ruxolitinb) and T cell checkpoints.

2. KEYWORDS:

Virotherapy
oHSV – Oncolytic Herpes Simplex Virus
MPNST – Malignant Peripheral Nerve Sheath Tumor
TGFβ – Transforming Growth Factor Beta
Ruxolitinib
PD-1 – Programmed cell Death protein 1

3. ACCOMPLISHMENTS:

What were the major goals of the project?

Specific Aims (specified in proposal)	Timeline	Percentage of completion
Aim 1. Compare viruses	Months	
Task 1.1 Therapeutic efficacy	1-6	100%
Task 1.2 Permissivity	1-6	100 %
Task 1.3 Immune cell modulation	3-9	100 %
Task 1.4 Cytokines/chemokines	3-9	100 %
Task 1.5 T cell subsets	9-12	Determined not to be relevant
Aim 2. TGFβ and PD-1 inhibitors	Months	
Task 2.1 Antitumor efficacy	12-18	100%
Task 2.2 T cell subsets	18-24	Determine not to be relevant
Task 2.3 Cytokines/chemokines	18-24	100%
Task 2.4 T cell effectors	24-30	Determine not to be relevant
Task 2.5 Dependence on TGFβR2 signaling	1-36	Determine not to be relevant
Task 2.6 TGFβ and PD-1 inhibition	24-36	100%

Specific Aims (continued)	Timeline	Percentage of completion
Aim 3. Ruxolitinib	Months	
Task 3.1 TGFβ and IL-10 expression	6-12	100%
Task 3.2 TGFβ and IL-10 loss of function	12-36	100%
Task 3.3 Virus production/persistence	12-18	100%
Task 3.4 Antiviral T cells	18-24	100%

What was accomplished under these goals?

Task 1.1: Determine the relative therapeutic efficacy of different oHSV constructs in immunocompetent mouse models of MPNST. We set out to compare the efficacy of the oHSVs HSV1716, T-VEC, and C134 in two immunocompetent mouse MPNST models, designated #5NPCIS and 67C-4. In our previous annual reports, we presented data from the efficacy study conducted with the #5NPCIS model that suggested each oncolytic herpes virus could elicit a small, but statistically significant improvement in overall survival compared to vehicle control. We have since been able to complete similar efficacy studies in mice bearing 67C-4 tumors, an MPNST model which until recently was difficult to establish in suitable numbers of mice. Figure 1A shows the treatment regimen employed by these studies, wherein #5NPCIS or 67C-4 tumors were treated with three intratumoral injections of oHSV (1e8 plaque-forming units per dose) once they had reached a size of 200-300 mm^3 in volume as determined by caliper measurements. Figure 1B shows individual #5NPCIS tumor growth curves for mice treated with HSV1716, T-VEC, C134 or a vehicle control. Figure 1C shows the impact of oHSV treatment on the overall survival of the mice in this study. HSV1716 and C134 treatment resulted in a slight, but statistically significant increase in overall survival relative to the vehicle control group ($p = 0.009$ and $p = 0.01$ respectively). There were no long-term survivors and no survival advantages for any particular virus over the others. We observed similar results with the 67C-4 model of MPNST (Figure 1D and 1E), however only the C134 virus produced a slight, yet statistically significant ($p \leq 0.05$) survival benefit over the vehicle control. Altogether, oncolytic herpes virus constructs had a marginal but statistically significant survival benefit as a monotherapy in immunocompetent mouse models of MPNST.

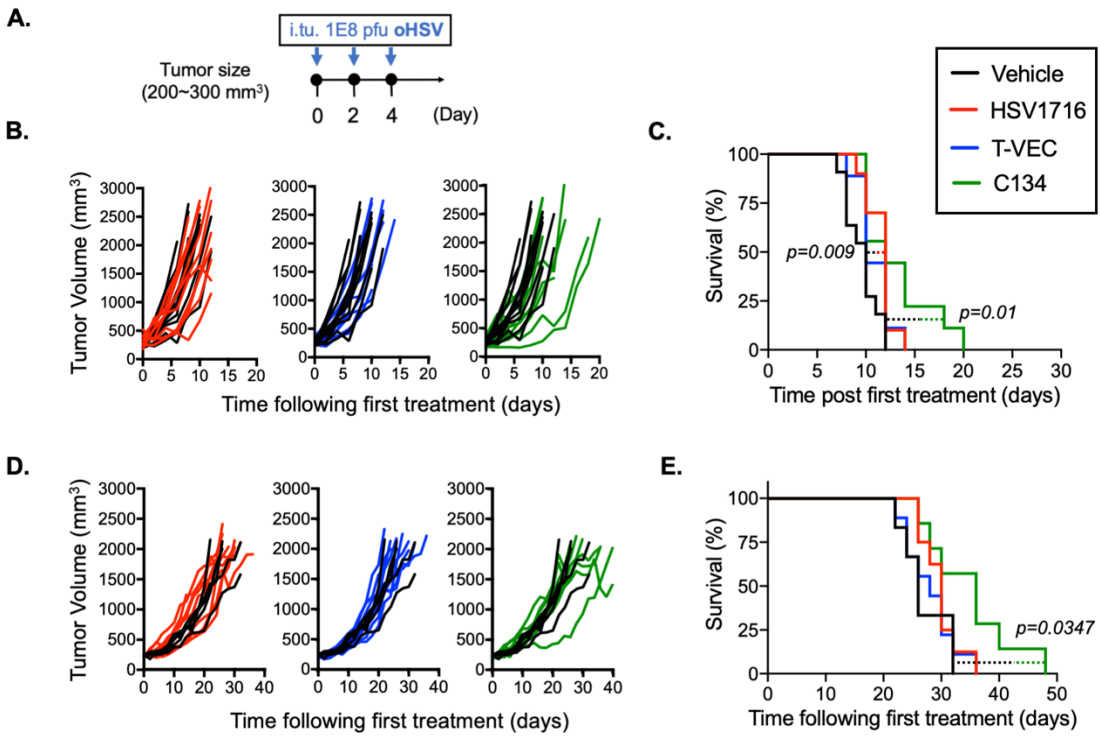

Figure 1. Oncolytic herpes virotherapy has a modest impact on survival in immunocompetent mouse models of MPNST. A.) Dose scheduling of mice implanted with #5NPCIS or 67C-4 tumors. The mice were treated with three intratumoral 1e8 PFU doses of HSV1716, T-VEC or C134 or an equivalent volume of PBS. B.) Individual tumor volumes of #5NPCIS tumor-bearing mice following treatment. C.) Kaplan-Meier survival curve of mice displayed in the previous panel. HSV1716 and C134 treatment produced a slight, but statistically significant enhancement on overall survival in the #5NPCIS model. D.) Individual tumor volumes of 67C-4 tumor-bearing mice. E.) Kaplan-Meier survival curves of 67C-4 mice showing benefit with C134 treatment. Statistical significance was assessed using the log-rank test.

Task 1.2: Measure the permissivity of mouse MPNSTs to each oncolytic herpes virus. As part of our comparison process, we wanted to determine if there were any differences in replication rates (permissivity) among the oHSVs following infection of mouse MPNST cell lines and tumors. For the in vitro experiments, we infected 67C-4 and #5NPCIS cells with HSV1716, T-VEC or C134 at a multiplicity of infection (MOI) of 0.5 plaque-forming units of virus per cancer cell. We then collected the infected cells at the listed timepoints and quantified the amount of virus produced with plaque assays (Figure 2A). For these in vitro studies, we noted that T-VEC appears to have the greatest permissivity, as it alone showed a small, but steady increase in the amount of infectious virus that could be recovered over time in both 67C-4 and #5NPCIS. HSV1716 and C134 on the other hand showed the opposite trend. We also conducted this study using a lower MOI of 0.05 pfu and observed similar trends (not shown).

To see if these observations held true in our mouse models, we implanted 67C-4 or #5NPCIS tumors on the flanks of immunocompetent mice and treated them with a single intratumoral 1e8 pfu

dose of virus. These animals were then sacrificed 3, 24, 48 or 72 hours later and their tumors were collected and processed to allow for quantification of virus by plaque assay (Figure 2B). In 67C-4 tumors, oHSV titers dropped steadily over the course of 72 hours regardless of which virus had been administrated. We also noted decreasing virus titers in the #5NPCIS tumors, although not to quite the same extent as that witnessed in 67C-4. Interestingly, we found that T-VEC had greater persistence in #5NPCIS compared to HSV1716 and C134, although this did not seem to have an impact on antitumor efficacy or animal survival (refer to Figure 1).

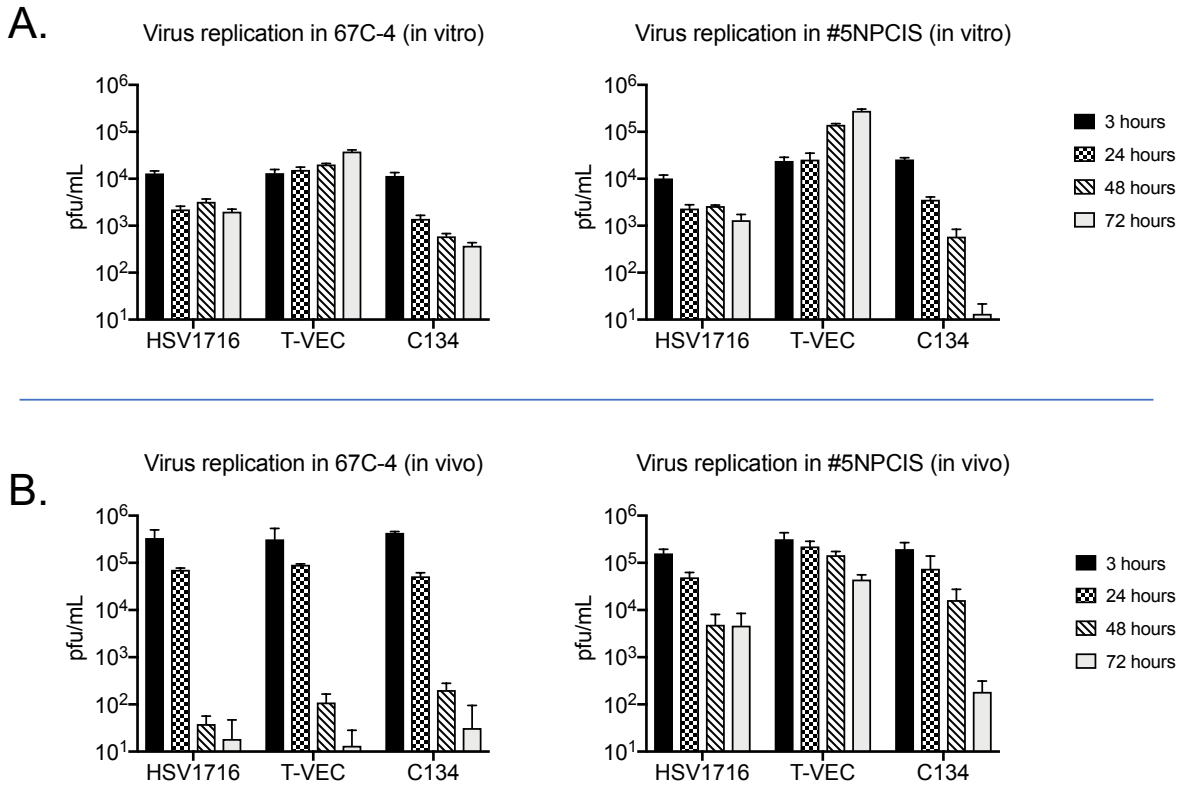

Figure 2. Average virus replication in 67C-4 and #5NPCIS A.) cell lines and B.) tumors. Each sample was run in quadruplicate. Error bars represent standard deviation.

Task 1.3: Compare viruses for their modulation of the immune cells within the tumor microenvironment. We know from previous studies that oncolytic herpes virus treatment promotes the influx of various immune effector cells to the tumor microenvironment. The purpose of task 1.3 was to determine if HSV1716, T-VEC or C134 treatment resulted in differential modulation of this response, which we would assess by using flow cytometry techniques to examine single-cell suspensions of processed tumors at various time points post infection. The immune infiltrate studies for #5NPCIS model are presented in its entirety below (Figure 3). All three oncolytic herpes viruses significantly increased total T cell infiltration (both CD4 and CD8) and reduced the frequency of immunosuppressive regulatory T cells. We also observed a small but significant T cell response

against a known tumor-associated antigen envelope, glycoprotein 70 (gp70), expressed universally in murine cancer cell lines but transcriptionally silent in normal tissues. A strong T cell response was observed against a major immunogenic virus peptide HSV1 glycoprotein B (gB). Although HSV1716 treated #5NPCIS mice had a statistically significant increase in T cells by day 7, relative to TVEC and C134, the difference is marginal. There was no statistically significant difference between T cell influx induced by each virus at day 11. Virotherapy did not alter the frequency of total macrophages at the time points tested. There was a significant increase in NK cells and neutrophils at Day 1, which decreased significantly at Day 7 but the differential infiltration upon each virus treatment was not significant. Altogether, all three oncolytic herpes viruses induce similar infiltration of immune cells in the #5NPCIS tumor microenvironment.

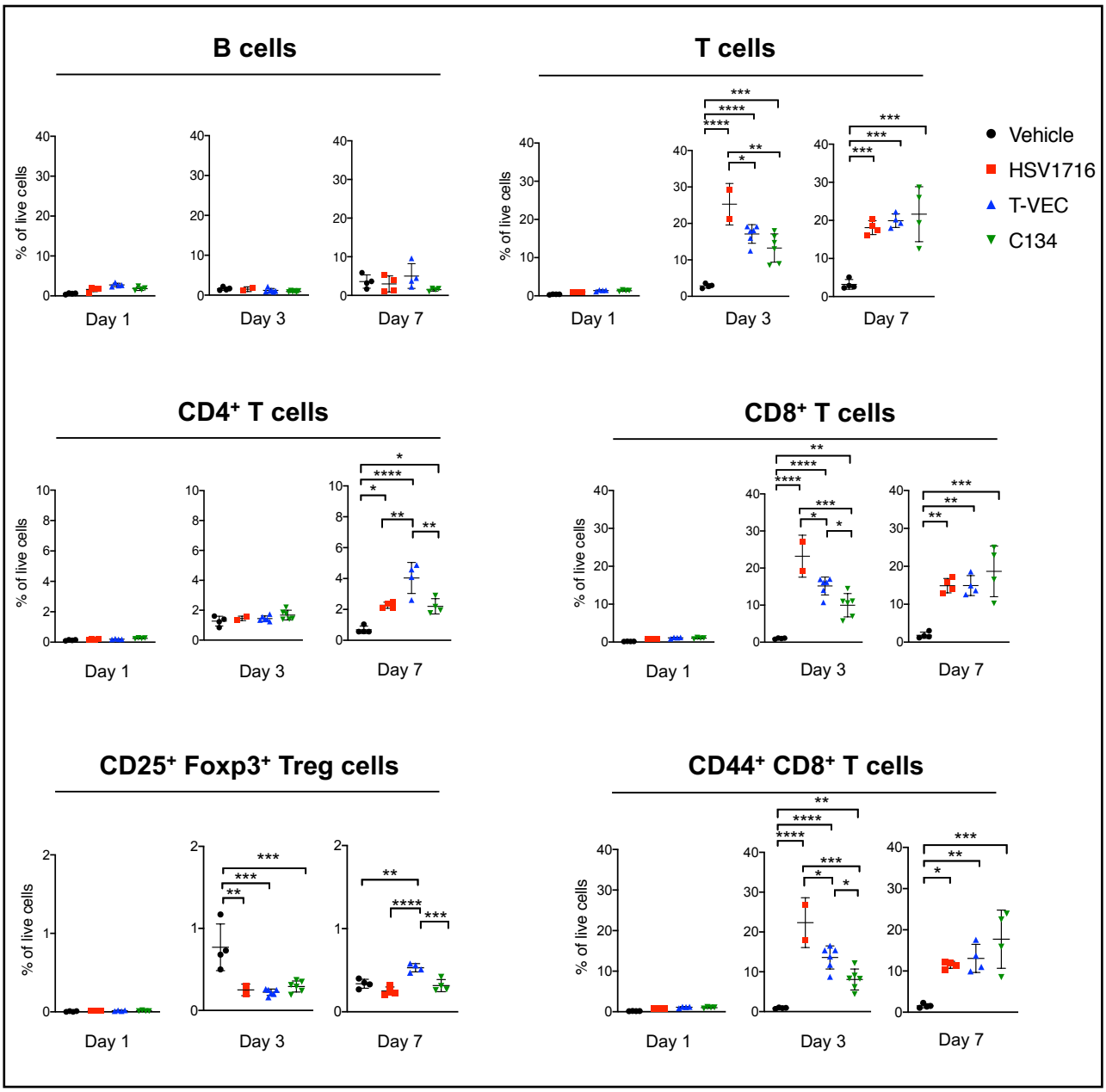

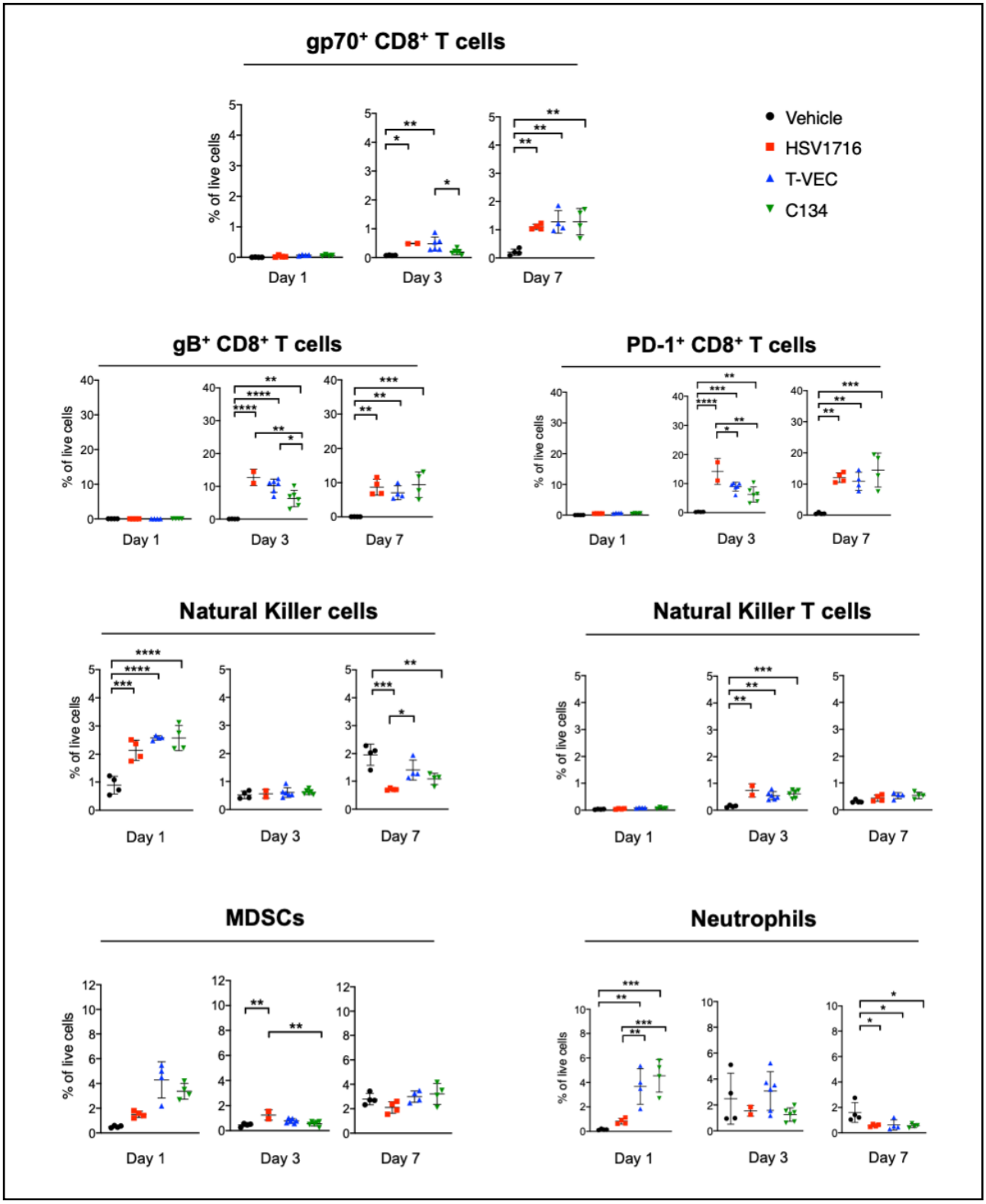
gp70+ CD8+ T cells
% of live cells
Day 1
Day 3
Day 7
Vehicle
HSV1716
T-VEC
C134
gB+ CD8+ T cells
PD-1+ CD8+ T cells
Natural Killer cells
Natural Killer T cells
MDSCs
Neutrophils

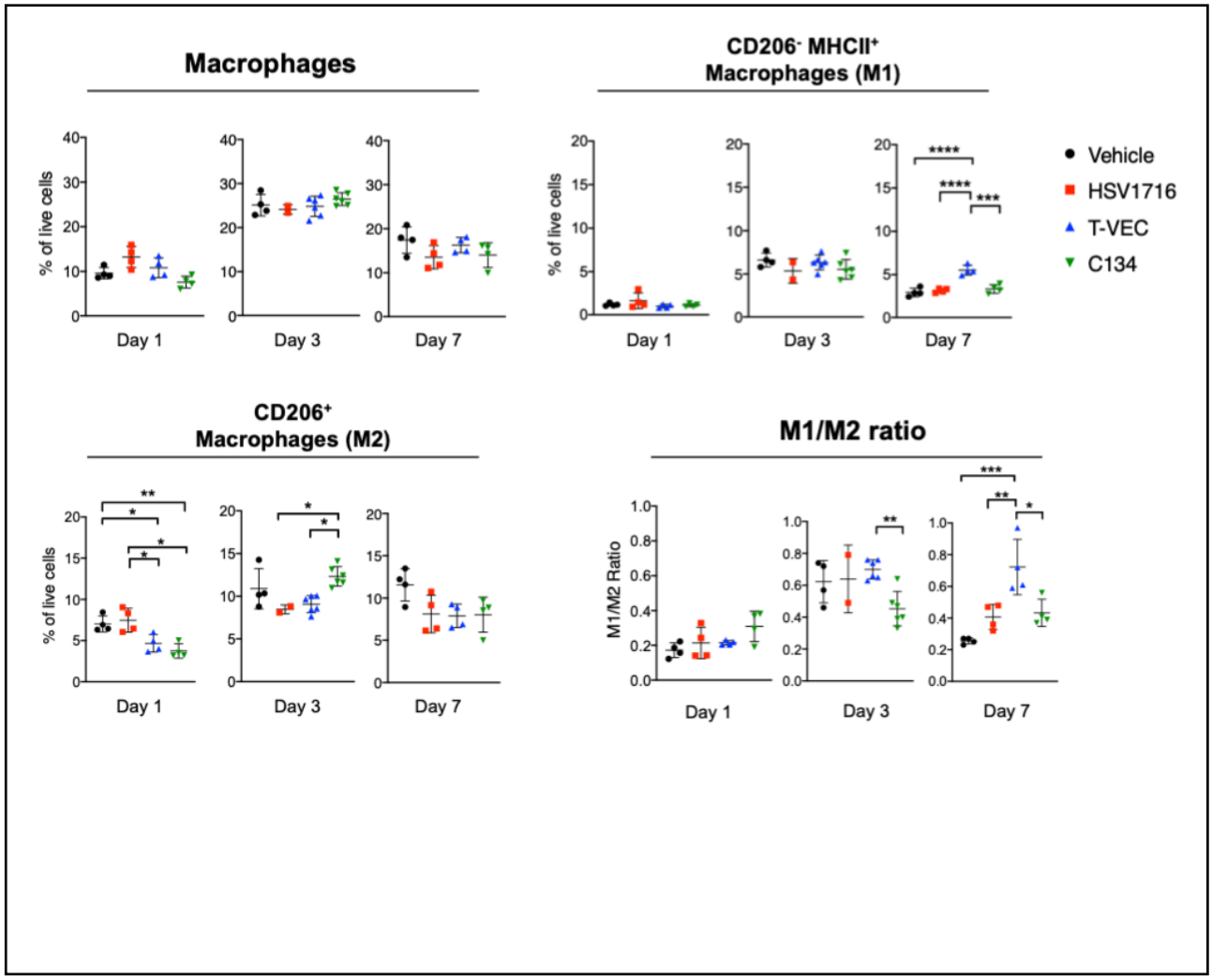

Task 1.4: Compare viruses for their induction of immunostimulatory cytokines and chemokines. Immunostimulatory and immunosuppressive cytokines in the tumor microenvironment influence T cell recruitment and function. The purpose of this task was to compare cytokine/chemokine expression profiles of infected MPNSTs and determine if there were any differences linked to the choice of oHSV. We accomplished this using the commercially available Proteome Profiler Mouse XL Cytokine Array (R&D Systems, Minneapolis, MN), which allowed us to detect and make qualitative assessments of the expression of 111 different mouse cytokines and chemokines in tumors treated three times with 1e8 pfu doses HVS1716, TVEC, C134 or a vehicle control. The cytokine and chemokine profile for the #5NPCIS model after treatment with the three oncolytic herpes simplex virus constructs are presented below (Figure 4). T cell chemo-attractants including CXCL9, CXCL10 and CCL21 increased after virotherapy. We also found a reduced expression of chemokines associated with regulatory T cell infiltration, CCL17 and CCL22. The viruses concurrently induced the expression of angiogenic factors angiopoietin-2 and feutin-A in #5NPCIS model. CCL2, CCL5 and M-CSF, the chemokines associated with macrophage infiltration, were also elevated after virotherapy. Overall, all three viruses had a similar profile with regards to their induction of cytokines and chemokines, with some differences amongst the viruses.

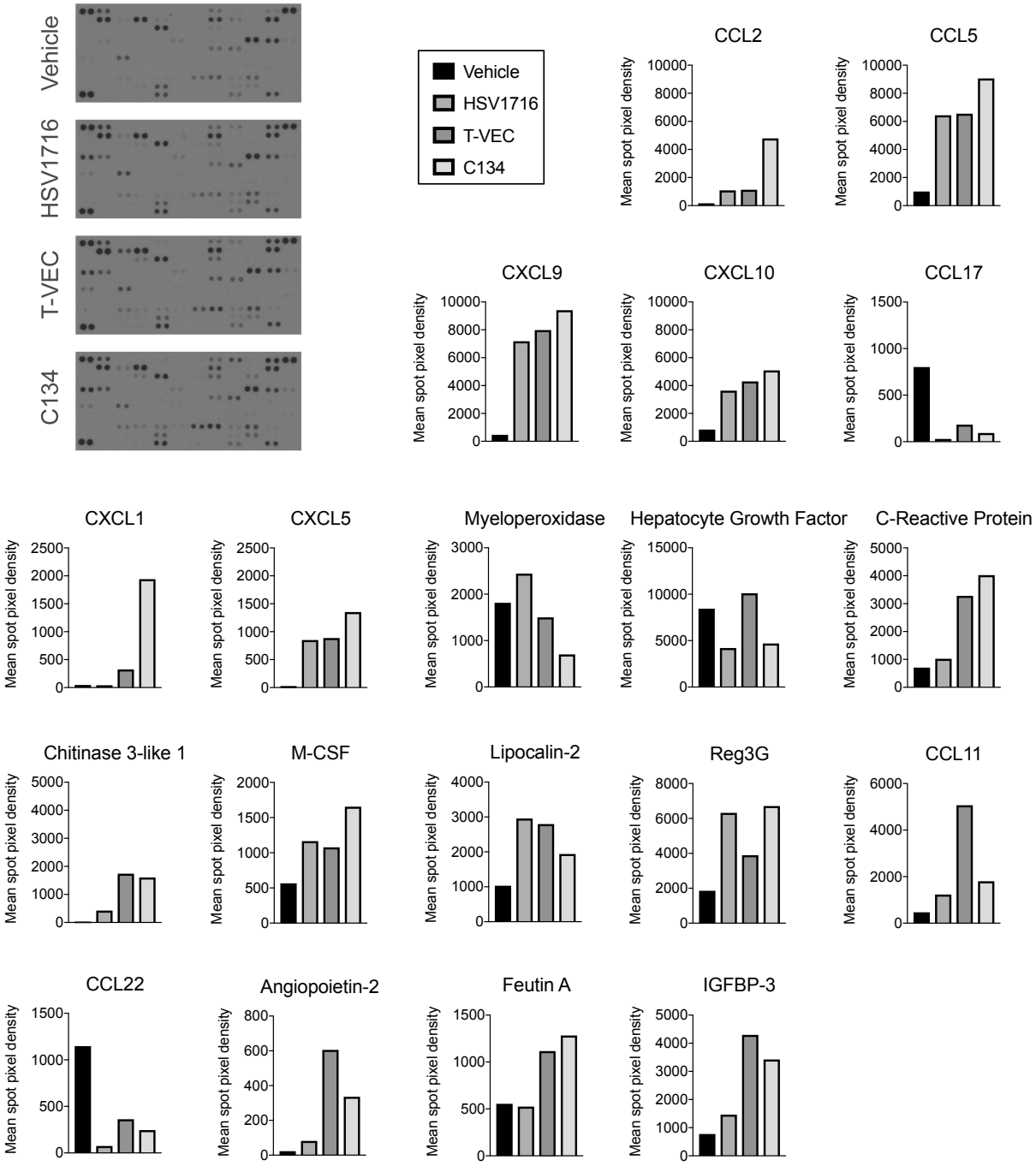

Figure 4. Proteome profile array data for #5NPCIS tumors treated with Vehicle, HSV1716, T-VEC, or C134. Tumors were treated three times with 1e8 pfu doses of respective virus or equivalent volume of vehicle control and harvested for analysis 24 hours after the final treatment. Densitometric quantification of listed cytokines/chemokines was performed with ImageJ software (National Institutes of Health, USA).

Task 1.5: Determine the dependence of virotherapy efficacy on T cell subsets. In this experiment, we originally proposed to systemically deplete $CD4^+$ and/or $CD8^+$ T cell populations in MPNST-bearing mice to gauge their relative contribution to the therapeutic response following oHSV infection. However, based on our data from task 1.1, we found these viruses were not effective as single agents. Thus, because of the lack of virotherapy efficacy, we did not conduct the depletion experiments because there was nothing to measure that would be dependent on T cells.

Task 2.1: Measure the effect of TGFβ inhibition on the antitumor efficacy of herpes virotherapy in mouse models of MPNST. The purpose of this task was to combine the oncolytic viruses compared in the first series of tasks with A8301, a small molecule inhibitor of the immunosuppressive cytokine TGFβ. These efficacy studies are similar to those described in task 1.1, however in addition to virus, each treatment group also received 6 mg/kg doses of A8301 administered intratumorally every other day. A schematic of the treatment regimen and the various treatment groups are shown in figure 5A. Kaplan-Meier survival curves and individual tumor volumes for the #5NPCIS model are shown in figure 5B and 5C, respectively. We again noted that there were no long-term survivors and no survival advantages for any particular virus over the others, however we did find that A8301 treatment by itself produced a slight survival advantage over the vehicle control ($p = 0.047$).

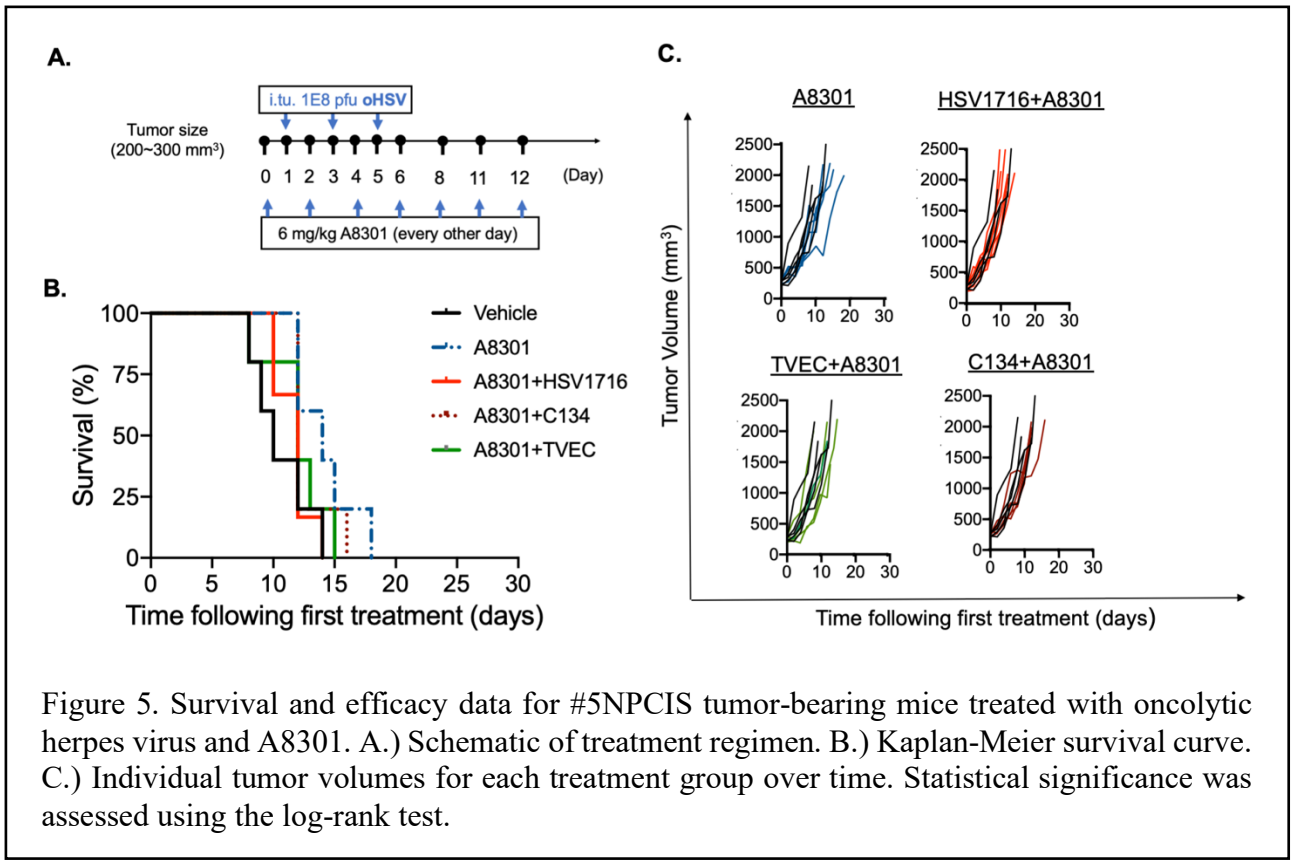

Figure 5. Survival and efficacy data for #5NPCIS tumor-bearing mice treated with oncolytic herpes virus and A8301. A.) Schematic of treatment regimen. B.) Kaplan-Meier survival curve. C.) Individual tumor volumes for each treatment group over time. Statistical significance was assessed using the log-rank test.

Task 2.2: Determine the effect of TGFβ inhibition on the influx of T cell subsets and their activation following virotherapy. In this experiment, we originally proposed to assess the modulation of intratumoral immune cells following treatment with the combination of oncolytic herpes virus and TGFβ inhibitor A8301. Since A8301 treatment had no significant survival advantage in combination with virotherapy, based on the data obtained from task 2.1, we decided that it would not be relevant to proceed with this study.

Task 2.3: Determine the effect of TGFβ inhibition on intratumoral expression of T cell chemokines. The purpose of this task was to compare cytokine/chemokine expression profiles of MPNST tumors treated with the combination of each oncolytic virus and the TGFβ inhibitor A8301. Similar to task 1.4, we utilized Proteome Profiler Mouse XL Cytokine Arrays (R&D Systems, Minneapolis, MN) to assess the expression of 111 different mouse cytokines and chemokines in #5NPCIS tumors treated three times with 1e8 pfu doses of oHSV interspersed with three 6 mg/kg doses of A8301. The tumors were collected for analysis 24 hours after administering the final dose of virus. In general, all three viruses stimulated one or more cytokines, with some differences amongst the viruses.

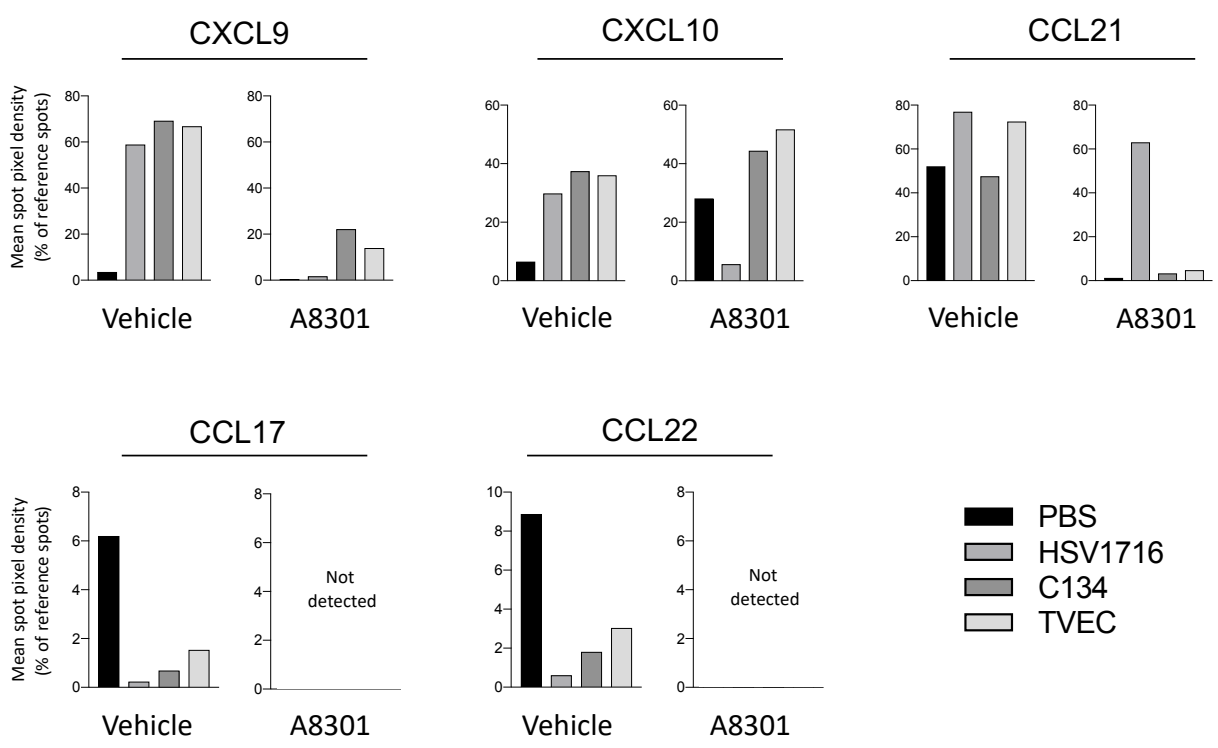

Figure 6. Densitometric quantification of T cell-associated cytokines and chemokines present in #5NPCIS tumors treated with oncolytic herpes viruses and A8301. CXCL9, CXCL10 and CCL21 are T cell chemoattractants whereas CCL17 and CCL22 are chemokines associated with T regulatory cells. Densitometric analysis was performed with ImageJ software.

Task 2.4: Test the role of T cell effectors in the enhancement of virotherapy due to TGFβ inhibition.

These experiments are similar to those described in task 1.5, where we originally proposed to systemically deplete $CD4^+$ and/or $CD8^+$ T cell populations in MPNST-bearing mice to gauge their relative contribution to the therapeutic response following oHSV and A8301 treatment. Unfortunately, the data from our efficacy studies (task 2.1) suggest that this combination therapy is also not effective against #5NPCIS tumors. As such, we decided these planned experiments were no longer relevant.

Task 2.5: Confirm the dependence of A8301 activity on TGFβR2 signaling in T cells. The purpose of this task was to confirm if A8301 enhanced virotherapy through the inhibitory effect on TGFβR2 complex, considering its potential to inhibit multiple receptors of the TGFβ family. Since A8301 treatment had no significant survival advantage in combination with virotherapy, we decided that it would not be relevant to determine/confirm if the inhibitor manifested its effect through a particular receptor.

Task 2.6: Determine if TGFβ inhibition is redundant to or complementary with PD-1 inhibition. We and others have shown that PD-1 inhibition can enhance the therapeutic potential of oncolytic virotherapy in some tumor models. This task was designed to not only determine whether this form of combination therapy was effective against our MPNST models, but also to examine if it could further benefit from the inclusion of TGFβ inhibition. Because we noted no significant differences amongst the oHSVs tested in earlier tasks, we selected T-VEC to use in these efficacy studies as it was the best characterized virus and the only oHSV to have obtained FDA approval. A schematic of the study design is shown in figure 7A. In short, #5NPCIS or 67C-4 tumor-bearing mice were treated with TVEC and/or A8301 as previously described. Subsets of #5NPCIS tumor-bearing mice were also given intraperitoneal injections of anti-PD-1 or control antibodies (250 μg) twice per week. Kaplan-Meier survival curves of #5NPCIS tumor model and plots of #5NPCIS tumor growth for each treatment group are shown in Figure 7B and 7C, respectively. We assessed statistical significance using the log-rank test, but found that none of the various combinations of therapy produced a survival benefit in #5NPCIS model. We also repeated these studies in 67C-4 mouse model of MPNST. Due to the relative difficulty of establishing 67C-4 tumors and the lack of efficacy observed in the #5NPCIS model, we decided to only compare T-VEC, anti-PD1 and A8301 triple combination therapy to a vehicle control. In contrast to #5NPCIS model, the triple combination therapy significantly prolonged survival in 67C-4 tumor model shown in figure 7D.

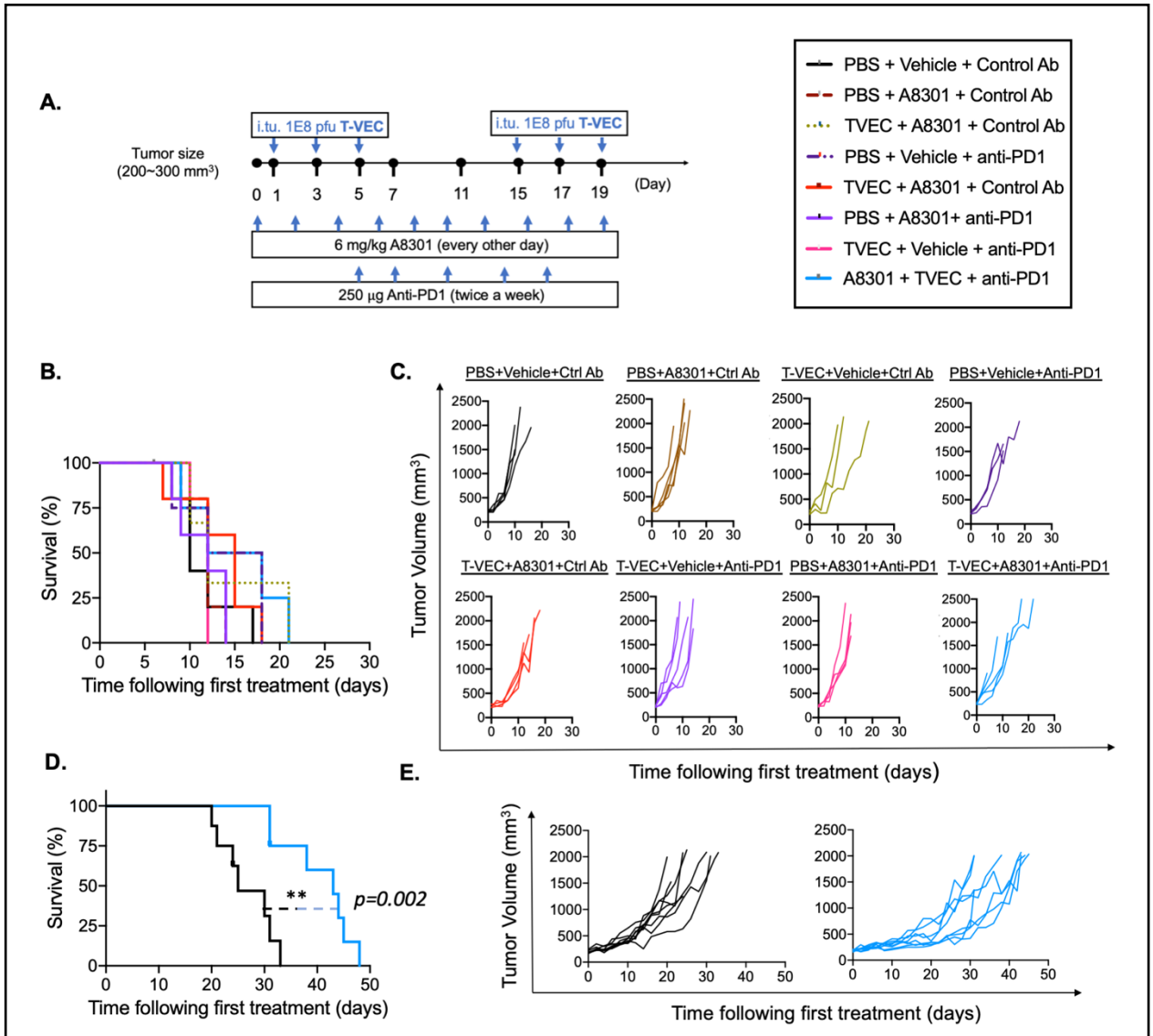

Figure 7. Combination of virotherapy, anti-PD1 and TGFβ inhibition significantly prolongs survival in 67C-4 tumor model but not in #5NPCIS tumor model. Survival and efficacy data of #5NPCIS and 67C-4 mice treated with a combination of T-VEC, A8301, and anti-PD-1 antibody. A.) Schematic of the treatment regimen. B.) #5NPCIS tumor model Kaplan-Meier survival curves. C.) Individual #5NPCIS tumor volumes for each treatment group over time. D.) 67C-4 tumor model Kaplan-Meier survival curves E.) Individual #67C-4 tumor volumes for each treatment group. Statistical significance of survival data was assessed using the log-rank test.

Task 3.1: Determine the effect of Ruxolitinib on TGFβ and IL-10 expression in mouse MPNST tumors. We found that Ruxolitinib enhances the antitumor effect of oncolytic HSV in mouse mdoels of MPNST using the C134 virus as shown in figure 8. We used qPCR in the 67C-4 model where tumor-bearing mice were treated for three consecutive days with 60 mg/kg with Ruxolitinib or an equivalent volume of a saline vehicle control, shown in figure 9. Ruxolitinib treatment not only significantly reduced expression of mouse TGFβ and IL-10, but also reduced expression of RIG-I, a pattern recognition receptor that typically acts to restrict herpes virus infection.

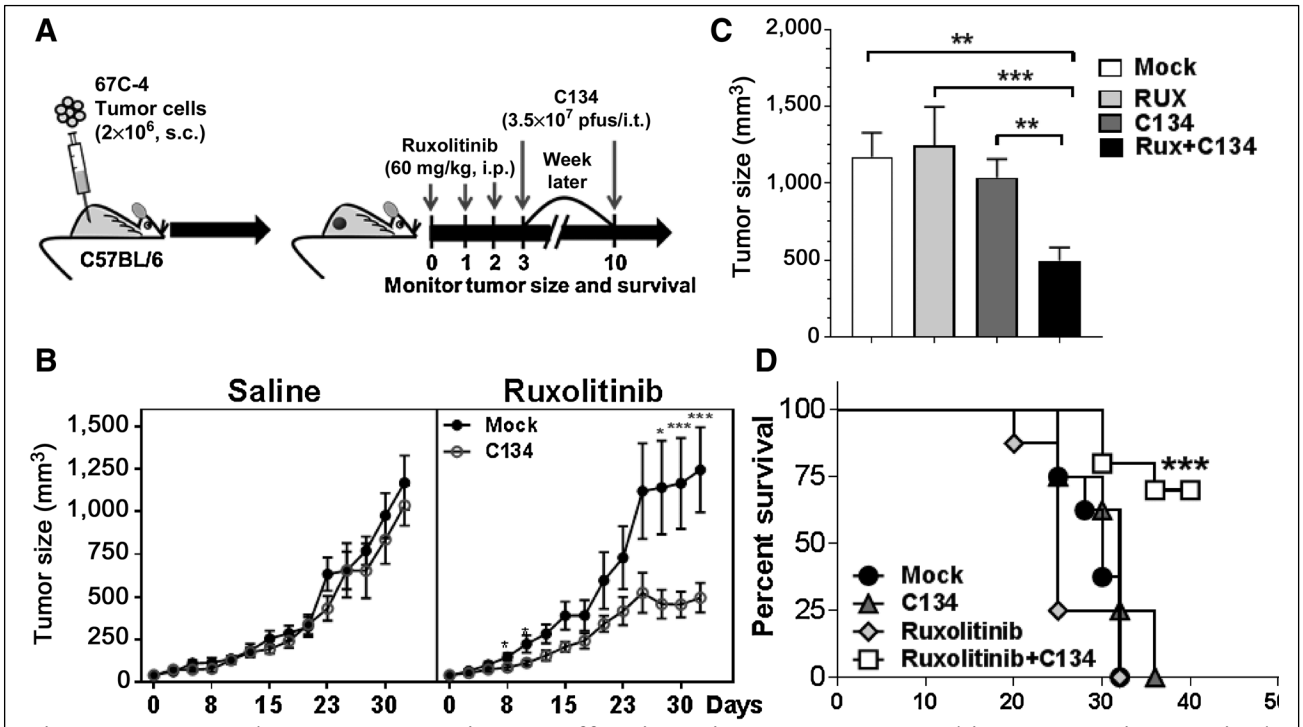

Figure 8. RUX enhances C134 antitumor effect in resistant MPNSTs and improves mice survival. A, Schematic of the experimental approach: C57BL/6 mice were implanted with 67C-4 cells subcutaneously in the flank. Tumor-bearing mice were randomized and divided into 4 treatment cohorts (mock, RUX alone, C134 alone, and combined RUX.C134) with 5mice/treatment group. Tumor-bearingmice were administered saline or RUX (60 mg/kg/d, i.p.) for 3 consecutive days and then treated with vehicle or 3.5x10e7 C134 intratumorally on days 3 and 10. B, Tumor growth was then measured by caliper-based tumor measurement (length x width x depth) over time. C, Tumor size differences (day 32) and D, mouse survival for the different treatment cohorts. Results, mean ± SEM of 5 mice/group. *, $P < 0.05$; **, $P < 0.01$; ***, $P < 0.001$; ****, $P < 0.0001$; n.s., not significant (two-way ANOVA). Survival was assessed using the log-rank test: the data are shown using Kaplan–Meier survival curves with median survival for each cohort included.

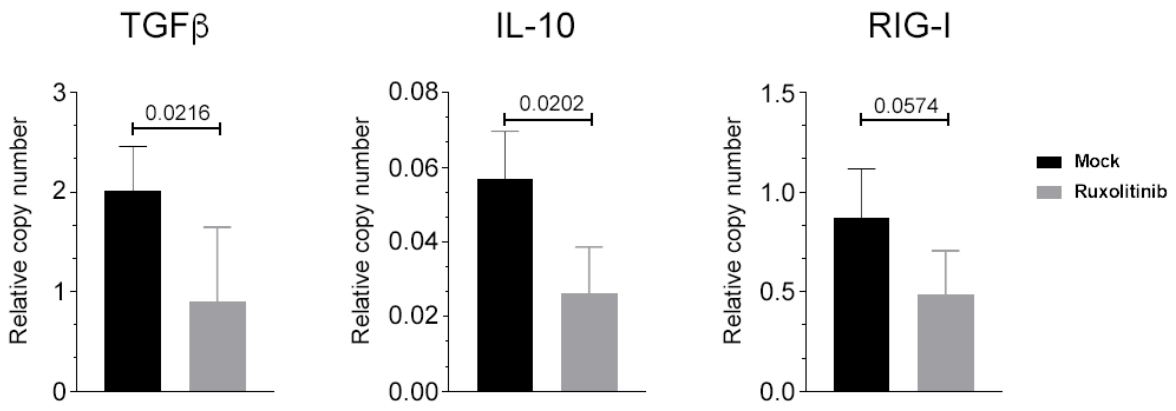

Figure 9. Ruxolitinib treatment reduces TGFβ and IL-10 gene expression in 67C-4 tumors. Mice were treated with 60 mg/kg Ruxolitinib or vehicle control and sacrificed 24 hours later for qPCR analysis (n = 4 per group). Gene expression data are presented as relative copy numbers. Statistical significance was determined using unpaired t-tests. Error bars represent standard deviation.

Task 3.2: Determine if inhibition of TGFβ and/or IL-10 accounts for the effects of Ruxolitinib on antitumor immunity. We were unable to find any evidence for a role of TGFβ or IL-10 in mediating the effects of Ruxolitinib on virus antitumor efficacy. Instead, we determined the effect of Ruxolitinib is most likely due to its role in inhibiting Jak/STAT signaling. We pursued these findings further and, by including supplemental funding from other agencies, we were able to demonstrate that other methods of inhibiting signaling through type I interferons recapitulated similar findings as Ruxilitinib in terms of increasing virus persistence and spread. Specifically, we found that inhibition of stimulator of interferon signaling (STING) in human MPNST cells also increased virus replication and spread. Because there is no clinically translatable "drug" that could be used to inhibit STING in vivo, we were unable to confirm these findings in any animal models.

Task 3.3: Test the effects of Ruxolitinib on intratumoral virus production and persistence. We used TaqMan qPCR to quantify virus from tumors harvested on days 1, 3 and 5 following treatment with C134 and Ruxolitinib or a vehicle control in the 67C-4 model, shown in figure 10. We found that Ruxolitinib increased the amount of virus recovered from tumors.

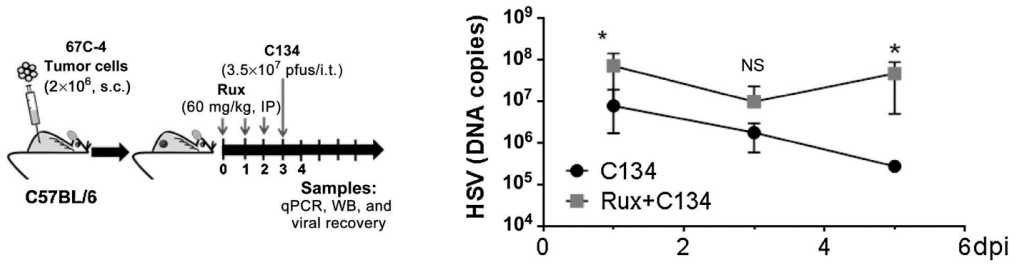

Figure 10. Ruxolitinib treatment increases the amount of C134 virus that can be recovered from 67C-4 tumors. Mice were treated three times with 60 mg/kg Ruxolitinib or vehicle control and sacrificed 1, 3 or 5 days later for qPCR analysis (n = 5 per group). Gene expression data are presented as relative copy numbers. Statistical significance was determined using two-way ANOVA. Error bars represent standard error of means. dpi = days post infection.

Task 3.4: Measure the effect of Ruxolitinib on the generation of anti-viral $CD8^+$ T cells. We found that Ruxolitinib increased the presence of activated T cells in the tumor and the T effector:regulatory ratio, suggesting the effects of the drug in combination with virus stimulates anti-viral and antitumor immunity (figure 11). We also used antibodies to deplete T cells and found that the effects of Ruxolitinib are dependent on CD8 T cells, as shown in figure 12.

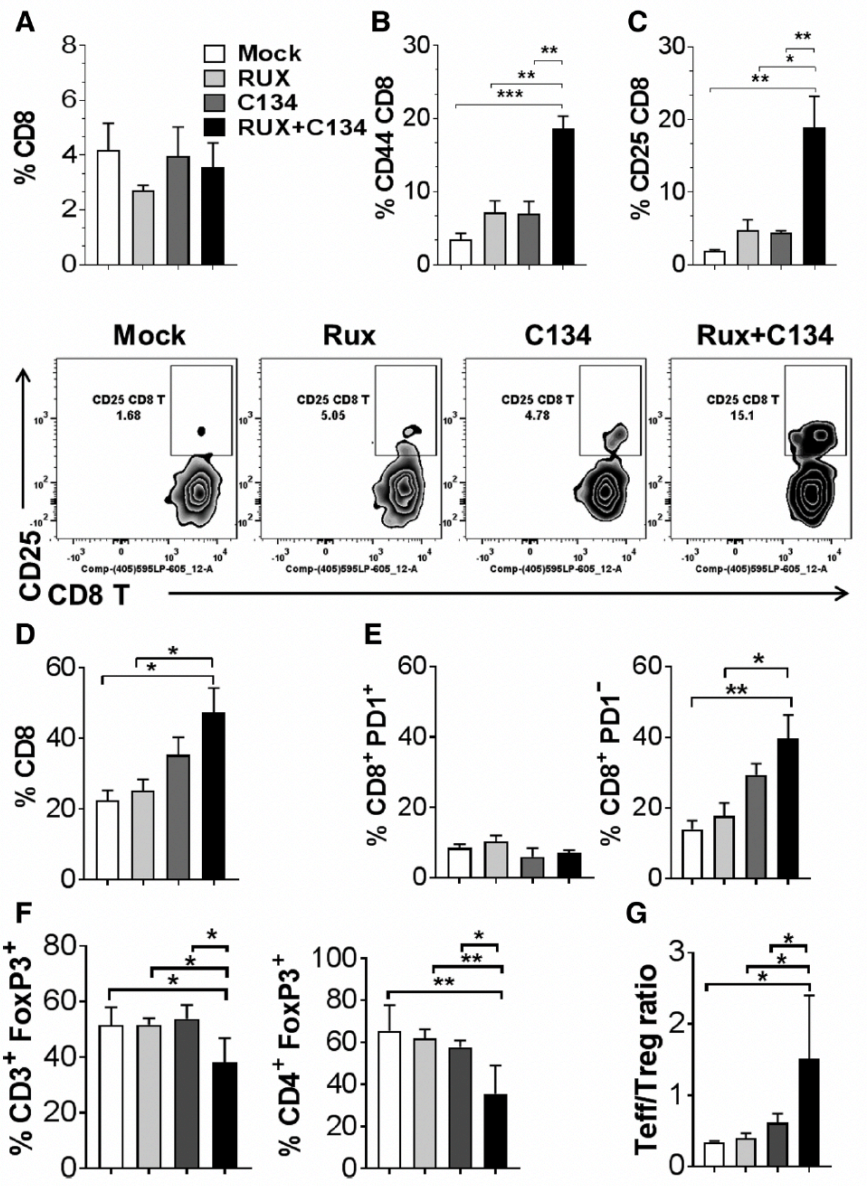

Figure 11. Combination therapy improves CD8. CTL activation in the tumor. As in Fig. 3A, C57BL/6 mice implanted with (2 x 10e6) 67C-4 cells subcutaneously were randomized and divided into 4 cohorts based on treatment regimen: mock, RUX alone, C134 alone, and RUX . C134. Tumors were harvested, processed into single-cell suspensions, and the TIL populations were analyzed. A, Overall CD8. T-cell populations day 6 of treatment (day 3 after viral treatment) were similar in all treatment cohorts RUX + C134 treatment increased CD8. T-cell activation as shown by (B) CD44 and (C) CD25 expression on the CD8. T cells (D6 of the overall study and D3 after oHSV treatment). Representative flow cytometry plots below show CD25 expression on CD8. T cells from the different treatment cohorts. D, On day 10 (day 7 after viral treatment), tumors were harvested, processed into single-cell suspensions, and CD8. T lymphocytes were analyzed by flow cytometry to assess CD8. T-cell population differences. E, PD-1 (+) and PD-1 (-) T-cell population percentages; F, FoxP3 expression on T-cell subsets, and G, the ratio of CD8. to CD4. FoxP3. in the TILs from our different treatment cohorts are shown. Results, mean $\pm$ SEM of 5 mice/group.*, $P < 0.05$; **, $P < 0.01$; ***, $P < 0.001$; ****, $P < 0.0001$; n.s., not significant (two-way ANOVA).

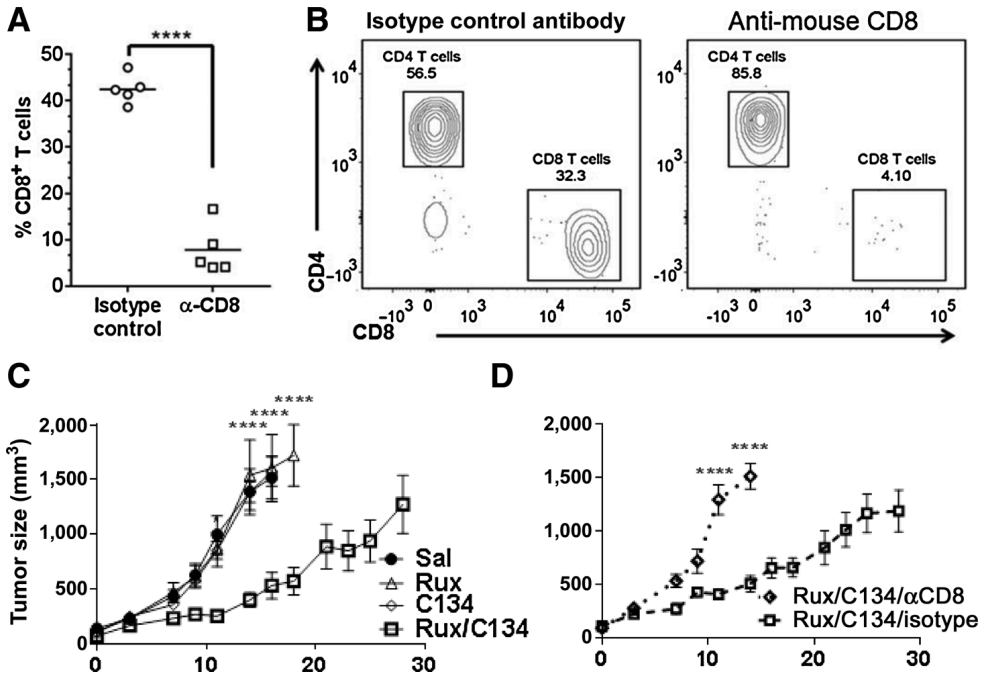

Figure 12. CD8+ T cells contribute to the efficacy of RUX + C134 combination therapy. C57BL/6 mice were implanted with (2 x 10e6) 67C-4 cells subcutaneously in the flank. Tumor-bearing mice were randomized into 4 treatment cohorts each with 10 tumors (mock, RUX, C134, and RUX + C134) with 5 mice/cohort. Mice were administered RUX (60 mg/kg, i.p.) for 3 consecutive days and then treated with 3.5 x 10e7 C134 i.t. at day 3 and 10. Mice were randomized and then treated with equimolar Ig anti-CD8a or isotype control every other day starting with the second dose of RUX. A, CD8. T-cell depletion confirmation by flow cytometry of peripheral blood in the anti-CD8a and isotype control groups. B, Representative flow cytometry plot from the Ig anti-CD8a and isotype control cohort. C and D, Tumor growth was measured by caliper and recorded (length x width x depth) over time in the 6 treatment cohorts. C, Mock (Sal)-, RUX-, and C134-treated cohorts were indistinguishable, similar to earlier studies; combination RUX . C134 reduces tumor growth. D, Combination therapy reduces tumor growth in the isotype-treated control but is ineffective in the CD8a-depleted cohort. Data were analyzed by two-way ANOVA with the Sidak multiple comparisons test. Results, mean $\pm$ SEM of 5 mice per group. *, $P < 0.05$; **, $P < 0.01$; ***, $P < 0.001$; ****, $P < 0.0001$; n.s., not significant (two-way ANOVA).

What opportunities for training and professional development has the project provided?

The project is helping provide the foundation for the graduate studies of Siddhi Nath Paudel, a Ph.D candidate in Dr. Cripe's lab.

How were the results disseminated to communities of interest?

We published a total of 5 manuscripts supported by this work, including 3 primary research articles and two review articles (see section 6 below), that are all available to the public for downloading (open access).

What do you plan to do during the next reporting period to accomplish the goals and objectives.

This is the final report for this project as described in our original grant proposal. We hope to incorporate the remainder of our unpublished findings into another manuscript for publication in the future. Because the unpublished results were largely negative (very little antitumor efficacy), we anticipate incorporating the results with other results we will obtain in related projects in order to tell a "publishable story."

4. IMPACT:

What was the impact on the development of the principal discipline(s) of the project?

Our data show that all three viruses are very similar in their activity in the murine MPNST models, though T-VEC may show a slight advantage based on increased replication in the cells. Unfortunately, we were not able to show that any combination of therapy is effective in affecting the #5NPCIS model. We did observe that the triple combination therapy of virus, anti-PD1, and anti-TGFβ slows the rate of tumor growth in 67C-4 model, though we did not observe tumor regressions. In addition, we found that virus plus Ruxolitinib slows 67C-4 tumor growth due to T cell infiltration/activation, but also did not induce tumor regressions. Our experience with these mouse models is not unlike the experience in human NF1 patients with MPNST, which are not very responsive to systemically administered treatments such as chemotherapy. We plan in future grants to propose to test other treatment approaches. Eventually, we hope to devise an effective treatment plan based on our mouse MPNST studies, at which point we will translate our findings into clinical trials in human patients.

The study also had an impact on other work in the laboratory. We used the baseline findings of activity of the C134 virus in MPNST cells as a jumping off point to develop, using funding from other sources, a strategy to leverage virus expression of "self proteins" to break tolerance to those proteins when they are overexpressed on cancer. For example, we were able to break tolerance to EphA2 in 67C-4 tumor-bearing animals using a virus that expresses EphA2. In a glioma model (CT2A) we were able to induce actual tumor regressions, but in the MPNST 67C-4 model the effect was only to slow tumor growth. These findings were recently published in Ghonime et al., JITC 2021. It will be interesting to test the combination of therapies used in this DOD-funded project with this "self tolerance-breaking" virus.

What was the impact on other disciplines?

Nothing to report.

What was the impact on technology transfer?

Nothing to report.

What was the impact on society beyond science and technology?

Nothing to report.

5. CHANGES/PROBLEMS:

Changes in approach and reasons for change

Nothing to report.

Actual or anticipated problems or delays and actions or plans to resolve them

Nothing to report.

Changes that had a significant impact on expenditures

Nothing to report.

Significant changes in use or care of human subjects, vertebrate animals, biohazards, and/or select agents

Significant changes in use or care of human subjects

This project does not involve human subjects.

Significant changes in use or care of vertebrate animals

There are no changes to report regarding our use of vertebrate animals.

Significant changes in use of biohazards and/or select agents

There are no changes to report regarding our use of biohazards and/or select agents.

6. PRODUCTS:

- **Publications, conference papers, and presentations**

Journal publications.

NOTE: ALL OF THE BELOW PUBLICATIONS ACKNOWLEDGE FEDERAL SUPPORT:

- Ghonime, MG, and Cassady, KA. Combination Therapy Using Ruxolitinib and Oncolytic HSV Renders Resistant MPNSTs Susceptible to Virotherapy. Cancer Immunol Res 2018, 6: 1499-1510.
- REVIEW: Hutzen B, Ghonime M, Lee J, Mardis ER, Wang R, Lee DA, Cairo MS, Roberts RD, Cripe TP, and Cassady KA. Immunotherapeutic Challenges for Pediatric Cancers. Mol Therapy Oncolytics 2019 Aug 28;15:38-48. doi: 10.1016/j.omto.2019.08.005. eCollection 2019 Dec 20. PMID: 31650024
- REVIEW: Hutzen B, Paudel SN, Naeimi Kararoudi M, Cassady KA, Lee DA, Cripe TP. Immunotherapies for pediatric cancer: current landscape and future perspectives. Cancer Metastasis Rev. 2019 Dec 11. doi: 10.1007/s10555-019-09819-z. PMID: 31828566
- Lee JM, Ghonime MG, Cassady KA. STING Restricts oHSV Replication and Spread in Resistant MPNSTs but Is Dispensable for Basal IFN-Stimulated Gene Upregulation. Mol Ther-Oncolytics 2019 PMID: 31650029 PMCID: PMC6804519 DOI: 10.1016/j.omto.2019.09.001
- Ghomine MG, Saini U, Kelly MC, Roth JC, Wang PY, Chen CY, Miller K, Hernandez-Aguirre I, Kim Y, Mo X, Stanek JR, Cripe T, Mardis E, Cassady KA. Eliciting an immune-mediated antitumor response through oncolytic herpes simplex virus-based shared antigen expression in tumors resistant to viroimmunotherapy. Journal for ImmunoTherapy of Cancer 2021;9:e002939. doi: 10.1136/jitc-2021-002939. PMID: 34599026

Books or other non-periodical, one-time publications.

Nothing to report.

Other publications, conference papers and presentations.

Nothing to report.

- **Technologies or techniques**

Nothing to report.

- **Inventions, patent applications, and/or licenses**

Nothing to report.

- **Other Products**

Nothing to report.

•

7. PARTICIPANTS & OTHER COLLABORATING ORGANIZATIONS

Name: Timothy Cripe, MD, PhD
Project Role: Principal investigator
Research Identifier:
Nearest person month worked: 2.0
Contribution to Project: Dr. Cripe helped conceive and plan the experiments and oversees the research related to Aims 1 and 2.
Funding Support: NIH, St. Baldrick's Foundation, Hyundai Foundation, Vyriad, Inc., institutional support

Name: Brian Hutzen, PhD
Project Role: Research scientist
Research Identifier:
Nearest person month worked: 2.0
Contribution to Project: Dr. Hutzen assists with the animal studies (efficacy, immune infiltrates, cytokine/chemokine expression) related to Aims 1 and 2.
Funding Support: DOD, CancerFree Kids Foundation, institutional support

Name: Pin-Yi Wang, PhD
Project Role: Research scientist
Research Identifier:
Nearest person month worked: 1.0
Contribution to Project: Dr. Wang assists with virus production for studies in Aims 1 and 2.
Funding Support: NIH, DOD, institutional support

Name: Chun-Yu Chen, PhD
Project Role: Research scientist
Research Identifier:
Nearest person month worked: 1.0
Contribution to Project: Dr. Chen runs the flow cytometry experiments related to this grant.
Funding Support: NIH, DOD, St. Baldrick's Foundation, institutional support

Name: Siddhi Nath Paudel
Project Role: Graduate research associate
Research Identifier:
Nearest person month worked: 6.0
Contribution to Project: Mr. Paudel conducts the animal studies (efficacy, immune infiltrates, cytokine/chemokine expression) related to Aims 1 and 2.
Funding Support: DOD, institutional support

Name: Kevin Cassady, MD
Project Role: Co-principal investigator
Research Identifier:
Nearest person month worked: 2.0
Contribution to Project: Dr. Cassady helped conceive and plan the experiments and oversees the research related to Aim 3.
Funding Support: NIH, Alex's Lemonade Stand Foundation, CancerFree Kids Foundation, institutional support

Has there been a change in the active other support of the PD/PI(s) or senior/key personnel since the last reporting period? Yes – some of the other supporting grants have been completed.

Cripe, Timothy

Completed:

N/A (Streby) 08/08/2016- 08/08/2019 0.72 calendar
United Therapeutics Corporation
Increasing ADCC in the tumor microenvironment with HSV1716 enhances ch14.18 anti-tumor efficacy

W81XWH1910371 (Cripe) 8/01/2019- 7/31/2021 2.40 calendar
Department of Defense
BiTE Gene Therapy to Augment Oncolytic Virotherapy

R21CA223104 (Cripe/Wang) 01/16/2019 – 12/23/2020 0.6 calendar
NIH/NCI
Improving Lytic Potency of Herpes Virus Cancer Therapeutics

R21CA237505 (Kudryashov) 4/12/2019- 3/31/2021 0.12 calendar
The Ohio State University/NIH
An innovative modular strategy for highly specific elimination of human osteosarcomas

Changes to Active:

U54CA232561 (Cripe/Mardis) 09/12/2019-08/31/2024 1.8 calendar
NIH
The Pediatric Ohio-New York Cancer (Peds-ONC) Immunotherapy Center

Cassady, Kevin

Completed:

N/A (Cassady) 10/01/16 - 12/31/18 1.8 calendar
Hyundai Foundation
Improving oncolytic virotherapy by suppressing Interferon Stimulated Gene over-expression in MPNST tumors

N/A (Cassady) 09/01/16 - 08/31/18 1.8 calendar
Alex's Lemonade Stand
Improving Immune-mediated oncolytic viral therapy: Engineering Tumor Vaccine Elements into the Virus

Changes to Active:

N/A (Markert/Cassady) 07/01/18 – 06/30/21 1.8 calendar
University of Alabama Birmingham/NIH/NCI
Oncolytic Immunotherapy using Chimeric HSV C134: A Phase I Trial and Establishment of Response Indicators in Recurrent Glioma Patients

U54CA232561 (Cripe/Mardis) 09/12/2019-08/31/2024 1.8 calendar
NIH
The Pediatric Ohio-New York Cancer (Peds-ONC) Immunotherapy Center

R21CA223104 (Cripe/Wang) 01/16/2019 – 12/23/2020 0.6 calendar
NIH/NCI
Improving Lytic Potency of Herpes Virus Cancer Therapeutics

What other organizations were involved as partners?

Nothing to report.

8. SPECIAL REPORTING REQUIREMENTS

COLLABORATIVE AWARDS:

QUAD CHARTS:

9. APPENDICES: